Hydrogen Interaction with a Ceria−Zirconia Supported Gold Catalyst. Influence of CO Co-adsorption and Pretreatment Conditions

Sebastián E. Collins,[‡] José M. Cíes,[†] Eloy del Río,[†] Miguel López-Haro,[†] Susana Trasobares,[†] José J. Calvino,[†] José M. Pintado,[†] and Serafín Bernal*[,†]

Departamento de Ciencia de los Materiales, Ingeniería Metalúrgica y Química Inorgánica, Facultad de Ciencias, Universidad de Cádiz, Campus Río San Pedro, E-11510 Puerto Real (Cádiz), Spain, and Instituto de Desarrollo Tecnológico para la Industria Química (CONICET, UNL), Güemes, 3450, S3000GLN Santa Fe, Argentina

Received: March 11, 2007; In Final Form: August 1, 2007

This work reports on the hydrogen interaction with a 3 wt % $Au/Ce_{0.62}Zr_{0.38}O_2$ (Au/CZ) catalyst prepared by deposition−precipitation. As deduced from X-ray powder diffraction, electron microscopy (scanning transmission electron microscopy−high-angle angular dark field and high-resolution electron microscopy), and CO volumetric/Fourier transform IR (FTIR) adsorption studies, the investigated catalyst shows a good metal dispersion. By combining FTIR spectroscopy and volumetric chemisorption studies, it is shown that upon treating the Au/CZ catalyst with 40 Torr of H_2 at room temperature a fast and very intense spillover effect occurs. As determined from the recorded isotherm, very high values of the apparent H/Au ratio (>8.0) and of the atomic hydrogen surface density (>11.0 H/nm^2) are reached. In parallel with this observation, the onset of a characteristic IR band at 2133 cm^{-1} shows the occurrence of significant support reduction with inherent appearance of Ce^{3+} species. Moreover, the simultaneous growth of the IR band at 1630 cm^{-1} due to molecular water strongly suggests that even at room temperature oxygen vacancies are also formed. Additional FTIR spectroscopy studies have shown that the hydrogen spillover is strongly inhibited by either co-adsorption of CO or a reducing pretreatment with flowing 5% H_2/Ar at 673 K. These deactivation effects, however, may be reverted by very mild regeneration treatments at room temperature.

Introduction

As stressed in a number of recent review papers,[1−7] the discovery by the second half of the 1980s of the extraordinary behavior of supported gold catalysts[8−10] and the huge amount of work following these pioneering studies[2] have obliged to a profound revision of the classic concepts about the catalytic properties of this metal. Traditionally considered as the least catalytically useful noble metal, it is presently acknowledged that if appropriately dispersed on the convenient support gold may become an extremely interesting catalytic material.[11−13]

Ceria-supported gold systems have received very special attention.[14−34] The main research effort on these materials has been focused on CO oxidation,[14,16,19,22,23,26,29] low-temperature water gas shift (WGS),[15,24,25,27,31−34] and selective oxidation of CO in presence of a large excess of hydrogen (PROX).[15,25,28,30] The hydrogen generation devices may thus be considered as a major potential application for these catalysts.[15,28] In most of these studies, the outstanding redox behavior of the ceria-related oxides[35, 36] is acknowledged to be a key feature justifying their interest as gold supports.[15,23,28]

To the present, pure CeO_2[14−34] and to a much lesser extent Ce−La[14,15,32,34] and Ce−Gd[15] mixed oxides have been the most investigated ceria-based supports. Despite the highly interesting redox properties of the ceria−zirconia-mixed oxides,[35,36] a few references are presently available on $Au/Ce_xZr_{1-x}O_2$ catalysts.[37−39]

In this work, we report on a 3% $Au/Ce_{0.62}Zr_{0.38}O_2$ catalyst. Our major goal is to gain some further information about the nature of its interaction with hydrogen. The influence of CO co-adsorption and of some thermo−chemical aging pretreatments on this interaction is also investigated. A number of reasons justify this study. First, it is presently well known that a deep knowledge of the H_2−ceria-based oxide systems,[40] and particularly, of the $H_2-Ce_xZr_{1-x}O_2$ one,[41] is critically important to fully interpret the redox chemistry of these materials. Second, in accordance with the available information, NM(Rh, Pt, Pd)/$Ce_xZr_{1-x}O_2$ may exhibit strong hydrogen spillover phenomena.[42−44] Though some experimental results, in particular temperature-programmed reduction (TPR) data[14] do also suggest the occurrence of similar effects in ceria-supported gold catalysts, no specific studies addressing this point have been reported as yet. Third, to gain information about the above-mentioned issues is certainly of interest to interpret in detail the role played by the support in some of the most relevant applications presently envisaged for ceria-based oxide-supported gold catalysts.

Experimental Methods

The gold catalyst with a 3 wt % metal loading was prepared by a deposition−precipitation procedure similar to that reported in ref 45. The mixed oxide support, $Ce_{0.62}Zr_{0.38}O_2$, was kindly donated by Grace Davison. The gold precursor was 99.99% $H[AuCl_4]$ (Alfa Aesar). The preparation procedure may be summarized as follows: 50 g of the support was suspended in 3 L of 5×10^{-3} mole L^{-1} aqueous solution of $H[AuCl_4]$ at room temperature. Then, urea was added until a concentration

* To whom correspondence should be addressed. E-mail: serafin.bernal@uca.es.
[†] Universidad de Cádiz, Campus Río San Pedro.
[‡] Instituto de Desarrollo Tecnológico para la Industria Química (CONICET, UNL).

10.1021/jp071968l CCC: $37.00
Published on Web 09/13/2007

of 0.42 mole L^{-1} was reached. Immediately after, the suspension was heated at 353 K and was kept at this temperature under vigorous stirring for 20 h in complete absence of light. Along this time, the pH remained stabilized between 8.0 and 8.5. The suspension was aged for 5 h at room temperature under stirring and filtered off. The resulting solid was washed several times with distilled water at room temperature until there was no evidence of chloride ions. Finally, it was dried overnight in an oven at 373 K, meshed at 125 μm, and stored in the dark under Ar until further use. This catalyst sample with a Brunauer/Emmett/Teller (BET) surface area of 62.8 m^2 g^{-1} will be hereafter referred to as fresh Au/CZ.

Fourier transform infrared (FTIR) spectra were recorded in the transmission mode on a Bruker, Vertex 70, instrument equipped with a DTGS detector. Typically, the spectra were obtained at 298 K by averaging 100 scans at a resolution of 4 cm^{-1}.

Self-supported wafers of 13 mm in diameter were obtained by pressing 40 mg of the fresh catalyst powder at 5 Ton/cm^{-2}. The disks were placed in a transmission infrared quartz cell with CaF_2 windows, which could be attached to a metallic high vacuum manifold equipped with a turbo molecular pump (residual pressure $<10^{-6}$ Torr). Likewise, the experimental device allowed the treatment of the sample disks under well-controlled thermo−chemical conditions. Temperatures ranging from 298 to 1173 K and partial pressures of the investigated gaseous reactants, H_2, O_2, and CO, ranging from 0.1 to 999.9 Torr, could be applied. For the latter purpose, high-purity gases were stored in glass balls and delivered in a controlled way during the pretreatment of the catalyst disks. Alternatively, in situ dynamic treatments under flowing gases could also be applied to the samples.

Prior to the FTIR experiments, the disks of the fresh catalyst or the bare mixed oxide support were heated in a flow of 5% O_2/He (60 cm^3 min^{-1}) at 523 K for 60 min, and then they were evacuated at the same temperature for 60 min, being finally cooled to 298 K under high vacuum.

Volumetric adsorption experiments, N_2 physisorption at 77 K, as well as H_2 and CO chemisorption were performed on a Micromeritics ASAP-2020 instrument. To guarantee a stable reference temperature throughout the whole chemisorption studies, isotherms were recorded at 308 K. The typical amount of sample used in these studies was 200 mg. Samples were pretreated as described above for the FTIR studies.

The TPR studies of both the $Ce_{0.62}Zr_{0.38}O_2$ support and the gold catalyst were performed on 180 mg of sample placed in a U-shaped quartz reactor. The evolved gases were analyzed with a Pfeiffer Thermostar quadrupole mass spectrometer. The 5% H_2/Ar flow rate was 60 cm^3 min^{-1}, and the heating rate was 10 K min^{-1}. The pretreatment applied to the sample was similar to the one adopted as standard in FTIR and volumetric studies. The only difference consisted of the substitution of the evacuation at 523 K (1 h) and further cooling under vacuum by a parallel routine in a flow of He (60 cm^3 min^{-1})

X-ray powder diffraction (XRD) studies were carried out on a Bruker instrument, model D8 ADVANCE. The diffractograms were recorded under the following conditions: CuK_α radiation; 2θ range, 5−85°; step, 0.05°; and the time per step, 30 s.

The Au/CZ catalyst pretreated as in the case of the TPR study described above has also been investigated by means of high-resolution electron microscopy (HREM) and high-angle annular dark field (HAADF) techniques. HREM images were recorded on a JEOL2011 LaB_6 electron microscope with 0.23 nm spatial resolution at Scherzer Defocus conditions. This value is adequate to image the internal structure of nanosized gold particles. HAADF images were obtained on a JEOL2010F instrument working in the scanning transmission electron microscopy (STEM) mode and using an electron probe of 0.5 nm of diameter at a diffraction camera length of 10 cm. This STEM−HAADF-imaging mode provides contrasts directly related to the average atomic number (Z) in the region under the electron beam. The difference in atomic number between Au ($Z = 79$) and the support cations ($Z_{Ce} = 58$, $Z_{Zr} = 40$) is large enough as to guarantee optimum imaging of gold nanoparticles with diameters even smaller than 1 nm. From the contrasts observed in both HAADF and HREM images, a simple discrimination of gold nanoparticles and support can be performed. In any case, the nature of the particles included in the size distribution was further confirmed by STEM−X-ray energy dispersive spectrometry nanoanalysis. Spectra corresponding to the individual particles were recorded using an Oxford INCA Energy TEM 200 system, which allows an energy resolution of 0.13 keV.

To avoid any contact with solvents, samples for electron microscopy studies were prepared by depositing small amounts of the catalyst powder directly onto holey-carbon coated Cu grids. Excess was removed from the grids by gentle blowing with a nozzle.

Results and Discussion

Preliminary Characterization Studies. *XRD and Electron Microscopy (HREM and STEM−HAADF) Studies.* To evaluate its metal dispersion, the Au/CZ catalyst has been characterized by means of XRD and electron microscopy (STEM−HAADF and HREM) techniques. XRD diagrams were recorded for the as-prepared fresh catalyst, as well as for the samples resulting from its further heating in a flow of 5% O_2/He, for 1 h at 523, 773, and 973 K. The corresponding diffractograms are reported in Figure 1 of the Supporting Information. Au diffraction peaks could only be detected in the samples heated at the highest temperatures. The oxidizing pretreatment at 523 K, the one adopted as standard in this work, would therefore lead to a well-dispersed phase with most of the gold mass consisting of nanocrystals smaller than 5 nm. This first indication was further confirmed and refined by the electron microscopy study, to be commented on below.

Figure 1 reports on the gold particle size distribution corresponding the Au/CZ sample submitted to the standard oxidizing pretreatment at 523 K. The distribution was determined by direct measurement of the size of 230 Au particles on both HREM and STEM−HAADF images. Representative examples of the micrographs used in this study may be found in Figure 2 of the Supporting Information. The distribution data were further processed to determine the average particle size, the cumulative metal dispersion, that is, the contribution to the dispersion of particles with size equal or smaller than a given value, and the total gold dispersion. All these parameters are also reported in Figure 1.

As deduced from Figure 1, our Au/CZ catalyst shows a narrow size distribution in which 95% of the gold particles have a size $\leq$3.0 nm. By contrast, particles larger than 5 nm represent less than 1% of the total distribution. In good agreement with these observations, an average particle size of 1.78 nm and a total metal dispersion of 0.53 (53%) were determined for the catalyst. Also worth of noting is that as deduced from the cumulative dispersion data reported in Figure 1, particles with size $\leq$ 2.0 nm represent more than 50% of the total dispersion with the contribution reaching the 89% for particles with size $\leq$ 3.0 nm. We should conclude, accordingly, that the gold

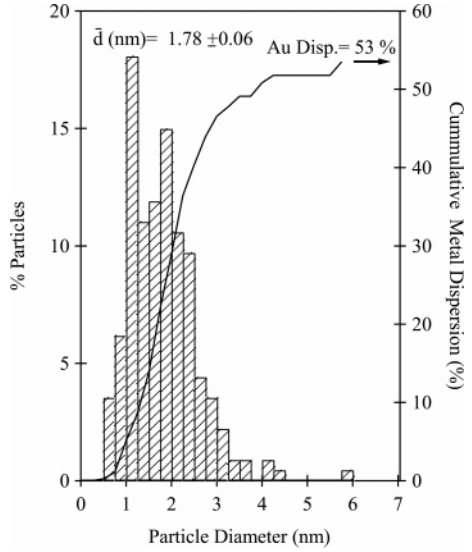

Figure 1. STEM−HAADF and HREM study of the gold particle size distribution corresponding to our Au/CZ catalyst submitted to the standard oxidizing pretreatment at 523 K. Data for the average particle size diameter, the cumulative metal dispersion, and the total metal dispersion as determined from the analysis of the size distribution are also reported.

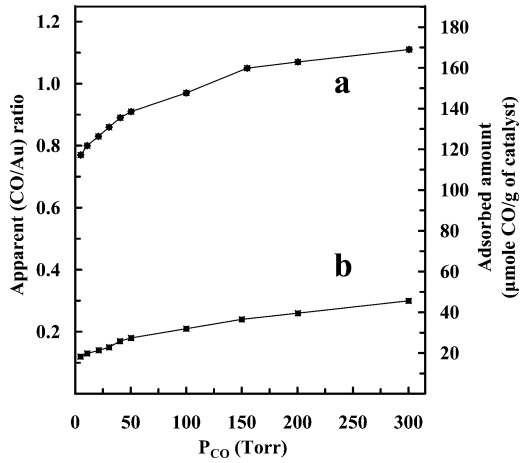

Figure 2. Volumetric adsorption of CO on the Au/CZ catalyst. Isotherms recorded at 308 K. (a) Catalyst heated in a flow of 5% O_2/He at 523 K (1 h) and further evacuated at 523 K (1 h). (b) Sample resulting from experiment (a) further evacuated for 30 min at 308 K.

surface chemistry of our catalyst is essentially determined by particles not larger than 3.0 nm.

Volumetric and FTIR Studies of CO Adsorption. We have also studied the CO adsorption on the catalyst submitted to the standard oxidizing pretreatment at 523 K. Volumetric chemisorption and FTIR spectroscopy techniques were combined in this study. As stressed in refs 46 and 47, a few volumetric studies are presently available on supported gold catalysts.

Figure 2 and Table 1 of the Supporting Information summarize the results of the volumetric study. Two isotherms were successively recorded at 308 K with the second one after 30 min evacuation at 308 K.

The bare CZ support was also studied by following exactly the same experimental routine as in the case of the Au/CZ sample. Data for the second of the two consecutive isotherms recorded for the mixed oxide are reported in Table 2 of the Supporting Information. If the second isotherms corresponding to the Au/CZ and CZ samples are compared, we may notice that for P(CO) ≤ 100 Torr the bare support represents a minor

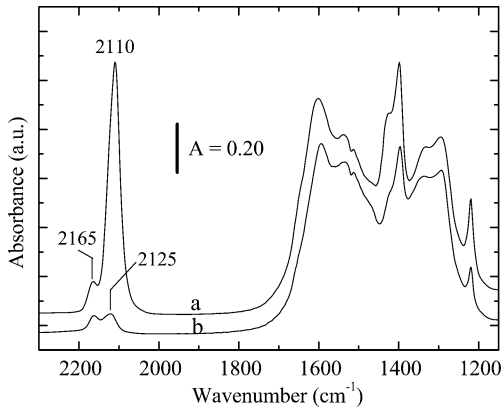

Figure 3. FTIR study of CO adsorption on the Au/CZ catalyst. (a) Spectrum corresponding to the fresh catalyst heated in a flow of 5% O_2/He at 523 K (1 h), further evacuated at 523 K (1 h), and finally treated with 100 Torr of CO for 30 min at room temperature. (b) Spectrum recorded after 30 min evacuation at 298 K of sample (a). Reference spectrum: pretreated catalyst prior the CO adsorption.

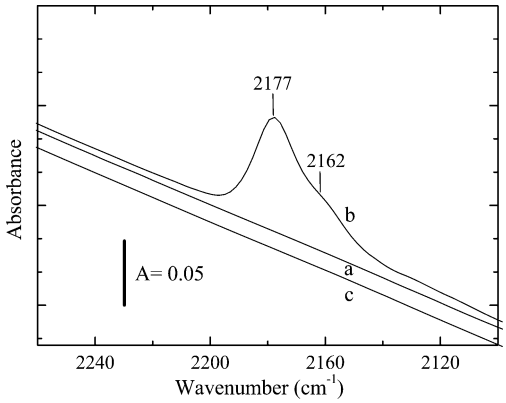

Figure 4. FTIR study of the CO interaction with the $Ce_{0.62}Zr_{0.38}O_2$ support heated in flow of O_2 (5%)/He at 523 K (1 h) and further evacuated at 523 K (1 h). (a) Spectrum of the as-pretreated sample. (b) Spectrum recorded after 30 min under 100 Torr of CO at 298 K. (c) Spectrum corresponding to sample (b) further evacuated for 30 min at 298 K.

contribution to the total amount of CO adsorbed on Au/CZ, not exceeding at most 20% of it.

The FTIR study of the CO interaction with the Au/CZ catalyst is reported in Figure 3. Two spectra were successively recorded: the first one, Figure 3, spectum a, under 100 Torr of CO and the second one, Figure 3, spetrum b, after 30 min evacuation at room temperature.

Figure 3, spectrum a shows the occurrence of strong absorption bands in two well-differentiated regions of the spectrum. Features corresponding to the stretching mode of CO (ν_{CO}) adsorbed on both Au and the cations of the support are observed in the 2000−2200 cm^{-1} range, whereas those assigned to carbonate species chemisorbed on ceria−zirconia appear in the 1100−1650 cm^{-1} region.

In accordance with the literature,[14,16,31,48] the band at 2110 cm^{-1} can be interpreted as due to linear CO chemisorbed on Au(0). The feature observed at 2165 cm^{-1} does not have an unequivocal interpretation.[16] CO forms interacting with oxidized gold[16] as well as with cations of the support, which are known to show bands in the range 2150−2200 cm^{-1},[49,50] are likely to contribute to this high-frequency feature. The latter contribution has been confirmed by a parallel study of CO adsorbed on the bare CZ support (Figure 4).

In good agreement with earlier studies on the CO interaction with CeO_2 and CeO_2−ZrO_2,[31,49,50] the second relevant region

of Figure 3, spectrum a clearly shows the formation of carbonate species. We should conclude, accordingly, that the support has a very significant contribution to the total amount of CO chemisorbed on the Au/CZ catalyst.

As deduced from Figure 3, spectum b, the effect of 30 min evacuation on the CO stretching and carbonate regions of the spectrum is very different. Bands occurring in the 2000−2200 cm^{-1} range almost completely vanish with the residual features at 2125 and 2175 cm^{-1} being reasonably interpreted as due to CO chemisorbed on neutral and oxidized forms of gold,[14] respectively. This proposal is supported by the spectrum reported in Figure 4 (spectrum c) in accordance with which the CO species adsorbed on the surface cations of the support are completely removed by a short evacuation treatment at 298 K. By contrast, the carbonate region of the spectrum reported in Figure 3 (spectrum a) is very slightly modified by the same evacuation treatment.

If the integrated absorptions for the two regions above in Figure 3, spectra a and b, are used as a rough indication of the quantitative effect of the evacuation treatment at 298 K, we may conclude that less than 10% of the forms responsible for the bands observed in the 2000−2200 cm^{-1} region remain chemisorbed, whereas less than 15% of those occurring in the carbonate region are desorbed. In other words, the second isotherm in Figure 2 would mainly account for the CO chemisorption on gold, and therefore it could be used to roughly estimate the (CO/Au) ratio. Thus, for 100 Torr, which is the partial pressure used in the FTIR study, a (CO/Au) value of 0.21 would be obtained (see Supportiong Information, Figure 2 and Table 1).

The proposal above, though reasonable, certainly implies rather crude assumptions on the compensation of the different adsorption phenomena contributing to the second isotherm, as well as on the absorption coefficients of the involved IR bands. In spite of the obvious limitations of this approach, it is worthwhile to notice that as will be discussed below the estimated CO/Au value is reasonably consistent with the metal dispersion value determined from the electron microscopy study reported in Figure 1.

It is presently acknowledged that CO adsorption on gold in addition to being weak mainly occurs on defective sites of its surface.[7,46,51] In spite of these singularities of gold, which certainly complicate the correlation of CO adsorption and metal dispersion data, a number of recent studies have provided some relevant clues for the analysis of this issue. Thus, Goodman et al,[52] by using infrared reflection absorption spectroscopy, have investigated the CO adsorption on the Au(110) (1 × 2) surface. They recorded a series of isobaric spectra from 1×10^{-8} to 1×10^{-4} Torr at temperatures ranging from 100 to 240 K. The highest CO coverage experimentally determined in ref 52 was 0.34. If the isosteric plot reported in ref 52 for this coverage is extrapolated to 308 K, which is the temperature at which the isotherms in Figure 2 were recorded, the resulting equilibrium partial pressure is found to be 20 Torr, which is lower than that applied in our estimate of the CO/Au ratio above (0.21 at 100 Torr). Moreover, as shown in refs 51 and 53 on Au/TiO_2 catalysts the CO adsorption enthalpies are significantly higher than those reported in ref 52 for the CO−Au(110) (1 × 2) system. If so, on supported gold catalysts the above-mentioned coverage of 34% might well be reached at equilibrium P(CO) even lower than 20 Torr.

Regarding the fraction of Au surface atoms involved in the CO adsorption, the 0.34 value reported for Au(110) (1 × 2)[52] may also be used as a reference. Likewise, it is reasonable to assume that in highly dispersed gold catalysts the surface concentration of adsorption sites may be similar, if not larger, than that deduced from ref 52 for Au(110) (1 × 2). If so, at the saturation limit a coverage of at least 0.34 may be reached on our Au/CZ catalyst. Taking into account the metal dispersion reported in Figure 1 (0.53) and assuming the above-mentioned coverage limit (0.34), a CO/Au ratio of 0.18 would be obtained for our catalyst. Though slightly smaller, this value is in fairly good agreement with that estimated from the volumetric study (0.21).

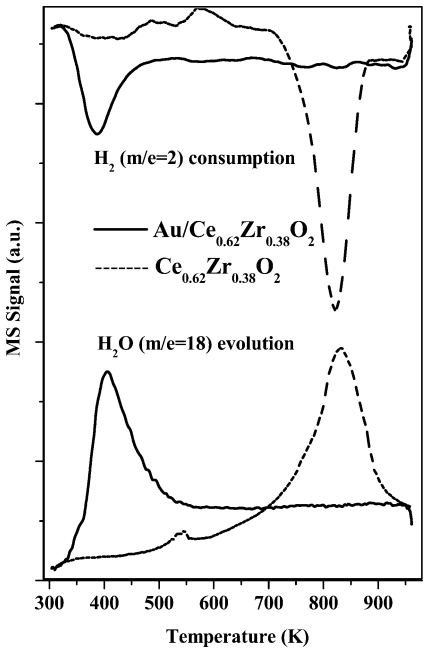

Figure 5. TPR-MS study of the Au/CZ catalysts and the corresponding CZ-mixed oxide support. Experimental conditions: amount of sample, 180 mg; 5% H_2/Ar flow rate, 60 cm^3 min^{-1}; heating rate, 10 K min^{-1}. Prior to the TPR runs, the samples were heated in a flow of 5% O_2/He at 523 K (1 h), then flushed with pure He at 523 K (1 h), and finally cooled to 298 K under flowing He.

Much lower estimates of CO/Au ratio values have recently been reported for a number of supported gold catalysts.[46] However, the experimental conditions applied in this study[46] were significantly different from ours. In particular, a pulse technique was used in ref 46. As deduced from the results discussed above, a very important part of the CO included in our estimate, which was eliminated by a short evacuation, cannot be measured by pulse experiments even if run, as is the case in ref 46, at temperatures well below 298 K. This probably explains the disagreement observed between our data and those reported in ref 46.

In conclusion, the results discussed above suggest that the volumetric study at room temperature of the CO adsorption on the Au/CZ sample investigated here, though not providing an accurate measurement of the CO/Au ratio, may be fruitfully used as a source of qualitative information about the gold dispersion of the catalyst.

TPR Studies. The preliminary catalyst characterization studies have also included a TPR investigation of the Au/CZ sample. Figure 5 depicts the H_2 consumption and H_2O evolution profiles for both the bare support and the Au/CZ catalyst. We may notice very significant differences between the traces recorded for the oxide and the supported gold samples. In good agreement with earlier TPR studies on ceria−zirconia mixed oxides,[54] the bare support shows broad H_2 consumption and H_2O evolution features centered at 840 K. By contrast, for the Au/CZ catalyst

the main H_2O (H_2) reduction peak is observed at 400 K. We should conclude, accordingly, that in the presence of the supported gold phase the reducibility of the mixed oxide is dramatically enhanced. Similar effects have earlier been reported for a number of ceria-containing gold catalysts,[14,34,55,56] as well as for several other ceria-[40] and ceria−zirconia-supported[41] noble metal systems. As recently shown[41] in the low-temperature range (T < 773 K), the reduction by hydrogen of ceria−zirconia-mixed oxides is a kinetically controlled process with the overall reaction rate being determined by the dissociative chemisorption of the reductant molecule. In the presence of Rh,[41] an alternative, much faster, mechanism consisting of the H_2 dissociation on the metal and subsequent transfer as atomic hydrogen onto the ceria−zirconia support (spillover) may operate, thus explaining the strong downward shift observed in the TPR trace for the Rh-containing sample. Our results in Figure 5, like those earlier reported on other ceria-containing gold catalysts,[14,34,55,56] clearly show that the effect of Au on the support reducibility is similar to that exhibited by Rh.[41] Accordingly, the mechanism explaining the role of Rh in the enhancement of the reducibility of Ce−Zr mixed oxides[41] may also operate in the case of the gold catalysts. This proposal is fully consistent with the FTIR and volumetric studies on the H_2 interaction with CZ and Au/CZ samples to be discussed below.

To summarize, our TPR study provides a first indication of the gold capability to activate the H_2 dissociation and spillover processes. Moreover, the analysis of Figure 5 clearly shows a very significant difference between the intensity ratio for the main H_2O and H_2 peaks in the bare support and the Au/CZ catalyst, much larger in the former case. This observation strongly suggests that for Au/CZ the H_2 trace only accounts for a part of the hydrogen consumption, which is the remaining part of it occurring at room temperature, before starting the TPR experiment.

Hydrogen Chemisorption Studies at Room Temperature. The H_2 interaction with the Au/CZ catalyst has been investigated by means of FTIR spectroscopy and volumetric chemisorption techniques. This rather unusual combination in gold characterization studies has proved to be a useful approach. Prior to running the experiments, the fresh catalyst was always submitted to the standard oxidizing pretreatment at 523 K followed by 1 h evacuation at 523 K.

FTIR Study of the H_2−(Au/CZ) System. Figure 6 summarizes the series of time-resolved spectra recorded for the Au/CZ catalyst under 40 Torr of H_2 at room temperature. The spectrum of the catalyst before any contact with H_2 is also included in Figure 6, spectrum a. As deduced from Figure 6, spectra b−g, under hydrogen pressure the OH stretching region is dramatically modified. Some bands observed in the reference spectrum, Figure 6 (spectrum a), disappear, whereas some new ones strongly grow up.

As summarized in Table 1, the spectrum reported in Figure 6 (spectrum a) consists of bands at 3772 and 3735 cm^{-1}, which may be assigned to OH groups linearly coordinated to Zr^{4+} cations (Zr-Type I) in different environments.[57,58] A feature at 3715 cm^{-1}, which in accordance with ref 57 may be interpreted as due to hydroxyl groups linearly coordinated to single Ce^{4+} cations (Ce-Type I), and the most intense one at 3663 cm^{-1} corresponds to bridged bidentate OH groups coordinated either to Ce^{4+} ions (Ce-Type IIA),[57] to Zr^{4+} ions (Zr-Type II),[57,58] or even to mixed Ce−Zr bridges.[57,60] Upon contacting the catalyst with H_2, the band at 3772 cm^{-1} vanishes immediately. Simultaneously, new bands are observed at 3682 and 3656 cm^{-1}. They may be assigned respectively to bridged hydroxyl species Ce-Type IIA and Ce-Type IIB, the latter corresponding to bibridged OH groups interacting with reduced forms of cerium, that is, Ce^{3+} species.[57,59] All these spectra are dominated by an additional, very broad, asymmetric feature centered at 3390 cm^{-1}, which clearly indicates the occurrence of H-bonded hydroxyl (OH_b) species.[57]

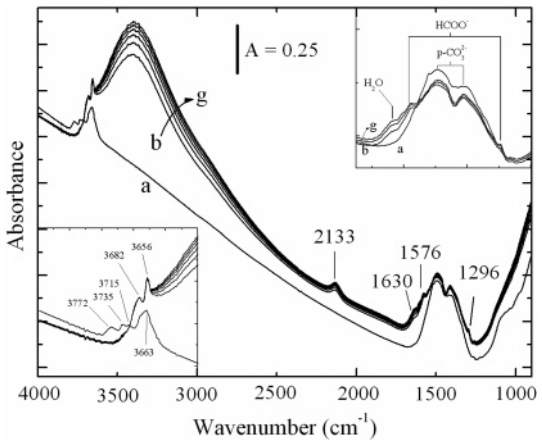

Figure 6. FTIR study of H_2-(Au/CZ) interaction. (a) Spectrum of the as-pretreated catalyst prior any contact with H_2. Spectra (b−g) were recorded, respectively, at 3, 5, 10, 15, 20, and 30 min after admission in the IR cell of 40 Torr of H_2 at 298 K. The bottom left and upper right insets report, respectively, on details of the ν(OH) and carbonate regions of the spectra.

We have also investigated the interaction of H_2 with the bare CZ support. As already noticed in the TPR study reported in Figure 5, the presence of gold deeply modifies the chemistry of the H_2−$Ce_{0.62}Zr_{0.38}O_2$ system. In effect, as shown in Figure 7, the evolution undergone by the spectrum of the oxide under 40 Torr of H_2 runs parallel to the one already described for the H_2−(Au/CZ). There is, however, a major difference; the very first indications of hydrogen adsorption on the bare support can only be observed at 473 K, and the band intensities progressively grow as the temperature is increased from 523 to 673 K. This behavior is fully consistent with the results reported in some very recent studies dealing with the hydrogen chemisorption on different ceria−zirconia samples.[41,60]

Despite the contradictory nature of the results reported in the literature on the capability of gold to activate the dissociative chemisorption of H_2 at room temperature,[61−63] the spectra reported in Figure 6 clearly show that if well dispersed on ceria−zirconia it is a highly active phase in promoting the hydrogen spillover. Moreover, the major changes in the FTIR spectra take place immediately after the contact with H_2 (Figure 6, spectrum b). This suggests that even at room temperature, the H_2 activation and subsequent transfer of atomic hydrogen to the support are very fast processes. Also in agreement with this proposal, our results indicate that 30 min H_2−(Au/CZ) interaction is long enough time as to reach the saturation of the support.

Noticeable changes may also be observed in the 1750−1000 cm^{-1} region of the spectra reported in Figure 6. The intensity of bands at 1492 and 1410 cm^{-1}, which may be attributed to residual polydentate carbonates chemisorbed on the ceria−zirconia mixed oxide,[49,50] decreases significantly. Simultaneously, a couple of bands at 1576 and 1296 cm^{-1}, due to formate species,[58] are developed. This implies that under hydrogen pressure in the presence of gold the surface carbonates on the support are also involved in the spillover process.

The analysis of Figure 6 has also allowed us to draw some interesting conclusions about the redox chemistry of the ceria−zirconia support. Two observations are relevant in this respect.

TABLE 1: Assignation of OH Surface Groups in Ceria−Zirconia-Related Oxide Systems

oxide/catalyst sample	ν(OH) cm^{-1} Zr−OH Type I	Zr−OH Type II	Ce−OH Type I	Ce−OH Type IIA	Ce−OH Type IIB	OH Type III	H−OH OH[b]	ref
ZrO_2-monoclinic	3768	3666						57, 58
ZrO_2-Tetragonal	3740	3660						58
CeO_2			3710	3662−84	3655	3560	ca. 3500	57
$Ce_{0.50}Zr_{0.50}O_2$ [a]			3711	3668−78	3648−50		ca. 3400	57
$Ce_{0.60}Zr_{0.40}O_2$ [b]	3780	3665	3710 (weak)	3665				60
$Ce_{0.62}Zr_{0.38}O_2$ (ox-500 °C)	3780	3670	3713	3668				this work
Au/$Ce_{0.62}Zr_{0.38}O_2$ (ox-523 K)	3772	3668	3715	3663				this work
$Ce_{0.62}Zr_{0.38}O_2$ (H_2−673 K)				3684	3638		ca. 3400	this work
Au/$Ce_{0.62}Zr_{0.38}O_2$ (H2−298 K)				3682	3656		3393	this work

[a] Spectrum recorded after three successive cycles of exposure to H_2 at 773 K (0.5 h each); spectrum acquired at 298 K under 13 Pa of H_2. [b] Spectrum recorded after three successive cycles of exposure to O_2 at 773 K (1 h each) followed by evacuation at the same temperature (1 h).

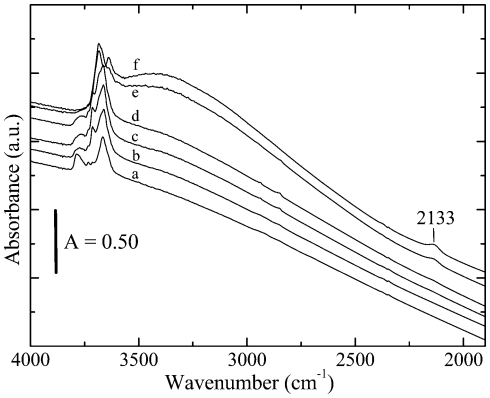

Figure 7. FTIR study of the H_2 interaction with the bare CZ support heated in a flow of O_2 (5%)/He at 673 K (1 h), further cooled to 398 K under the same oxidizing flow, and finally to 298 K under high vacuum. (a) Spectrum of the as-pretreated sample. Spectra (b−f) were recorded, respectively, after 30 min heating at 473, 523, 573, 623, and 673 K and further cooling to 298 K always under 40 Torr of H_2.

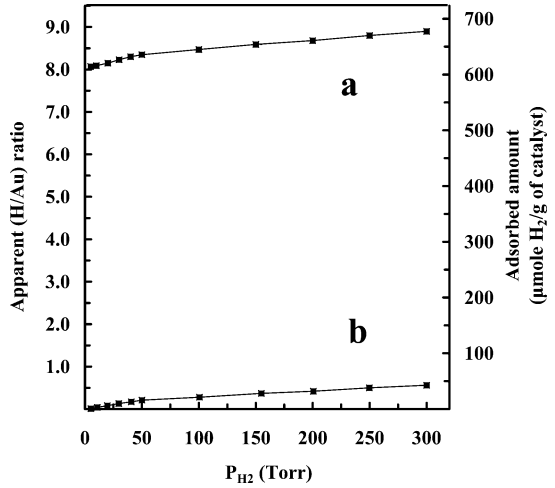

Figure 8. Volumetric adsorption of H_2 on the Au/CZ catalyst. Isotherms recorded at 308 K. (a) Catalyst heated in a flow of 5% O_2/He at 523 K (1 h) and further evacuated at 523 K (1 h). (b) Sample resulting from experiment (a) further evacuated for 30 min at 308 K.

First, the appearance and growth in Figure 6, spectra b−g, of a new band at 2133 cm^{-1}, which is interpreted as due to a forbidden electronic transition ($^2F_{5/2} \rightarrow {}^2F_{7/2}$) in Ce^{3+}.[64] This band may be used to monitor the redox state of the ceria−zirconia support.[60] Second, the development in spectra b−g of a band at 1630 cm^{-1} due to the bending mode of H_2O. The immediate formation of molecular water strongly suggests that even under the very mild reducing conditions of the experiment, anionic vacancies could be created in the ceria−zirconia lattice.

First reported for Rh/CeO_2,[65,66] it is presently well known that hydrogen spilled over ceria-containing oxides may induce two distinguishable reduction processes: reversible and irreversible processes. The reversible one is associated to atomic hydrogen chemisorbed on the surface of the oxide. This process may be reverted with inherent reoxidation of the support by simple evacuation.[66] By contrast, the irreversible reduction would imply the creation of oxygen vacancies with parallel formation of water. Consequently, a further evacuation of the catalyst would not modify the support redox state.[66] In the case of our H_2−(Au/CZ) system, the evolution of the Ce^{3+} band with the evacuation temperature suggests, in good agreement with the observations commented on above, that both reversible and irreversible reduction processes coexist.

Volumetric Study of the H_2−(Au/CZ) System. The hydrogen spillover has also been evaluated on quantitative bases. For this purpose, we have used a volumetric technique. The catalyst pretreatment was exactly the same as that applied in the FTIR study. Two hydrogen isotherms were successively recorded at 308 K. The second one was obtained after 30 min evacuation at 308 K. Figure 8 and Table 3 of the Supporting Information summarize the corresponding results. The amounts of chemisorbed hydrogen have been expressed as both apparent H/Au ratio (Figure 8, ordinate scale on the left) and μmole H_2 g^{-1} of catalyst (Figure 8, ordinate scale on the right). Regarding the first isotherm, there are a number of observations to be outlined. At 308 K, large amounts of hydrogen are chemisorbed by the catalyst. As shown in Figure 8 and Table 3 of the Supporting Information, at $P(H_2) = 40$ Torr the partial pressure used in the FTIR study, an apparent (H/Au) ratio as high as 8.3, is determined. Such a high (H/Au) value clearly shows the occurrence of a very strong spillover effect. If this amount is referred to the nm^2 of BET surface area of the catalyst, 11.7 H atoms nm^{-2} is obtained. By using as a reference the reported density of O^{2-} ions in the (111) plane, the most dense one of the $Ce_{0.63}Zr_{0.37}O_2$ mixed oxide,[67] the full surface coverage, would correspond to 8.2 H atoms nm^{-2}. The above-mentioned amount exceeds such a limit thus indicating, as already suggested by the observation of molecular water in our FTIR study, Figure 6, that some oxygen vacancies with inherent consumption of 2 H atoms per O^{2-} are created.

Two more observations are remarkable in relation to the isotherm depicted in Figure 8, scan a. First, the amount of chemisorbed hydrogen is very large even at the lowest partial pressure, (H/Au) = 8.1, at $P(H_2) = 5$ Torr. Second, at this point of the isotherm the apparent equilibrium is reached in less than 3 min. These two observations, which are fully consistent with the FTIR results reported in Figure 6, clearly indicate that at 308 K on the Au/CZ catalyst both the hydrogen adsorption on the metal and the spillover are fast processes.

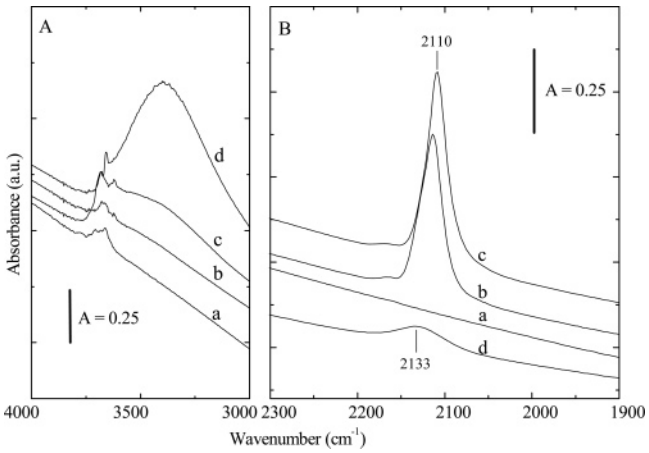

Figure 9. FTIR study of the influence of CO co-adsorption on the hydrogen spillover effect. Analysis of ν_{OH} (Panel A) and ν_{CO} (Panel B) frequency ranges. (a) Au/CZ sample submitted to the standard oxidation/evacuation pretreatment at 523 K. (b) Spectrum recorded 30 min after the admission of 10 Torr of CO in the cell. (c) Spectrum recorded 30 min after the addition of H_2 (40 Torr) without evacuating the preadmitted CO. (d) Spectrum recorded after 30 min interaction of 40 Torr of H_2 with the Au/CZ catalyst in the absence of CO. Figure 5 (spectrum g), is included for comparison.

Regarding the second isotherm, Figure 8, scan b, we may notice that the amount of chemisorbed hydrogen is much smaller, (H/Au) = 0.2, at $P(H_2)$ = 40 Torr. Likewise, the (H/Au) ratio progressively increases with $P(H_2)$. This suggests that at 308 K the spillover process is essentially irreversible, and therefore that in agreement with some recent theoretical studies,[68] atomic hydrogen forms weakly interacting with the dispersed metal phase could be involved in the second isotherm. These results are consistent with an adsorption process occurring on some specific, defective gold sites, rather than on the whole surface of the metal nanocrystals.[61,63]

Deactivation and Regeneration of the Hydrogen Spillover Effect. We have also investigated the influence of CO co-adsorption and of some thermo−chemical aging pretreatments on the hydrogen spillover phenomena. FTIR spectroscopy was the technique used in this study.

Effect of CO Co-Adsorption. To investigate this effect, a disk of the fresh catalyst was submitted to the standard oxidation/evacuation pretreatment at 523 K, Figure 9, spectrum a, then 10 Torr of CO was admitted in the IR cell, Figure 9, spectrum b. As already commented on in our analysis of Figure 3, the preadsorption of 10 Torr of CO significantly modifies two regions of the spectrum. The CO stretching range is dominated by a sharp band at 2110 cm^{-1}, which has been assigned to CO adsorbed on metallic gold sites.[14,16,31,48] This band is accompanied by a second much less intense feature centered at approximately at 2165 cm^{-1} to which contributions from CO adsorbed on both oxidized forms of Au and the support might well be expected to occur.[16] Changes in the carbonate region, not shown in Figure 9, may also be noticed. These changes are, however, very similar to those already reported in Figure 3. The co-adsorption experiment was completed with the admission in the cell of 40 Torr of H_2 without removing the pre-existing gaseous CO. A series of time-resolved IR spectra were then collected. For the sake of clarity, only one spectrum, which was recorded after a 30 min interaction with H_2, is reported, Figure 9, spectrum c. Figure 9, spectrum d, reproduces the spectrum already shown in Figure 6 (spectrum g), that is, that corresponding to 30 min H_2−(Au/CZ) interaction in the absence of CO.

Two major conclusions may be drawn from the analysis of Figure 9. First, upon comparison of spectra b and c, we may deduce that the CO stretching band at 2110 cm^{-1} is not significantly modified by the co-adsorption of hydrogen. This is so despite the relative partial pressures of CO (10 Torr) and H_2 (40 Torr), thus indicating that CO adsorption is stronger than that of hydrogen.[68] Second, the presence of CO inhibits the hydrogen spillover process very significantly. These two observations are consistent with the common nature of the gold sites involved in the adsorption of H_2 and CO. They are also consistent with a number of earlier studies in accordance with which both H_2[61, 63] and CO[7,46] adsorption would mainly take place on special low-coordination gold sites.

It could be argued, however, that the CO inhibition of the spillover effect might well be caused by the carbonate species formed during the CO pre-adsorption. To evaluate the feasibility of such a hypothesis, the catalyst pretreated with 10 Torr of CO was evacuated at room temperature for 30 min, and then 40 Torr of H_2 was admitted in the cell. Bands due to hydroxyl groups grew up rapidly with a spectrum almost identical to that reported in Figure 5, spectrum g, being recorded after 30 min exposure to H_2. As already shown in this work, upon short evacuation at 298 K the CO chemisorbed on gold is almost completely removed, whereas the carbonate species at the support are much less affected. We may conclude, accordingly, that the competitive nature of the CO and H_2 adsorption on gold, rather than the presence of carbonate species at the surface of the support, is responsible for the inhibition of the spillover effect. Also remarkable is that the perturbation induced by the coadsorbed CO may be reverted by simple evacuation at room temperature.

Effect of Prereduction at 673 K. We have also investigated the influence on the hydrogen spillover of a prereduction treatment at 673 K. A disk of the fresh Au/CZ sample was reduced in situ at 673 K (1 h) in a flow of 5% H_2/Ar, then it was evacuated at 673 K (1 h) and cooled to 298 K under high vacuum. After recording the spectrum of the reduced/evacuated sample, 40 Torr of H_2 was admitted in the IR cell, and the series of time-resolved spectra depicted in Figure 9 (spectra b−h) was obtained. As we may notice, after 30 min treatment with H_2 the $\nu(OH)_b$ region of the initial spectrum is very slightly modified. Therefore, the reduction/evacuation treatment at 673 K almost completely inhibits the spillover effect.

To evaluate the reversibility of the observed deactivation, the sample resulting from the experiment above was evacuated for 30 min at room temperature and treated with 40 Torr of O_2 for 30 min always at room temperature. Following this treatment, we may notice the complete disappearance of the band at 2133 cm^{-1} (see spectrum a in Figure 11). As already discussed, this feature may be used to monitor the redox state of the ceria−zirconia mixed oxide[60] with its absence suggesting the complete reoxidation of the support. Next, the sample was evacuated for 30 min at 298 K, and 40 Torr of H_2 was admitted again in the cell. Spectra b−e in Figure 11 account for the evolution of the sample during the 30 min following the H_2 admission. It is obvious that the applied reoxidation treatment has induced a very significant recovery of the hydrogen spillover with a progressive increase with time of the intensity of the OH stretching bands being observed. Likewise, the 1750−1100 cm^{-1} region of the spectra is modified, thus suggesting, as already deduced from the analysis of Figure 5, that the spilled over hydrogen does also interact with the carbonate species at the surface of the support. Finally, Figure 11 shows that under hydrogen pressure the characteristic bands of Ce^{3+} at 2133 cm^{-1}

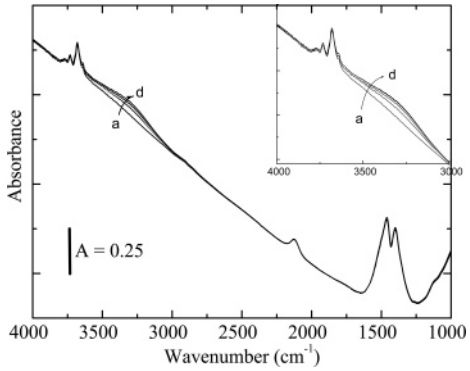

Figure 10. FTIR study of the hydrogen spillover effect in the Au/CZ catalyst reduced in a flow of 5% H_2/Ar at 673 K (1 h) and further evacuated at 673 K (1 h). (a) Spectrum of the as pretreated catalyst. Spectra (b−g), time-resolved series recorded during the 30 min following the admission of 40 Torr of H_2 in the IR cell.

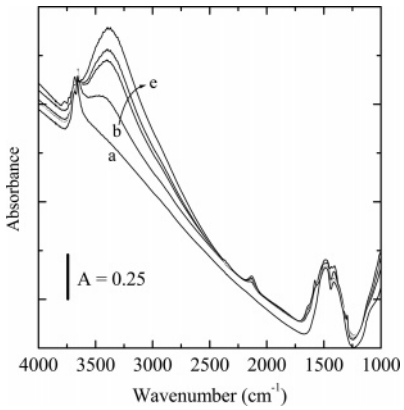

Figure 11. FTIR study of the hydrogen spillover effect in the Au/CZ catalyst reduced at 673 K (1 h), evacuated at 673 K (1 h), reoxidized at 298 K (0.5 h) with 40 Torr of O_2, and finally evacuated at 298 K (1 h). (a) Spectrum of the as pretreated catalyst. Spectra (b−e), time-resolved series recorded during the 30 min following the admission of 40 Torr of H_2 in the IR cell.

and molecular water at 1630 cm^{-1} reappear and grow up thus indicating the occurrence of a very significant support reduction.

It should be noticed, however, that a careful analysis of the spectra reported in Figure 11 shows that on the catalyst reduced at 673 K and further reoxidized at 298 K the spillover process is slower than in the case of the sample submitted to the standard oxidation/evacuation pretreatment at 523 K (Figure 6). A partial recovery of the spillover effect could only be achieved in the former case.

The concentration of oxygen vacancies at the surface of the oxide support must play a relevant role in determining both the rate and the amount of spilled over hydrogen. Therefore, the observed regeneration is very likely due, at least in part, to the support reoxidation induced by the oxygen treatment at 298 K.

To investigate the role of the gold phase in this recovery effect, some additional FTIR experiments were run. They were aimed at studying the eventual changes induced on the metal phase by both the reduction/evacuation treatment at 673 K and its further reoxidation/evacuation at 298 K. Figure 12 reports on this study. Spectra of CO (P_{CO} = 10 Torr) adsorbed on the Au/CZ catalyst submitted to the standard pretreatment on the sample reduced at 673 K, as well as on the latter catalyst further reoxidized at 298 K, are shown in Figure 11, spectra a−c, respectively. Some remarkable differences may be observed. By using spectrum a of Figure 12 as a reference, we may notice that the main CO stretching (ν_{CO}) band in spectrum b is shifted

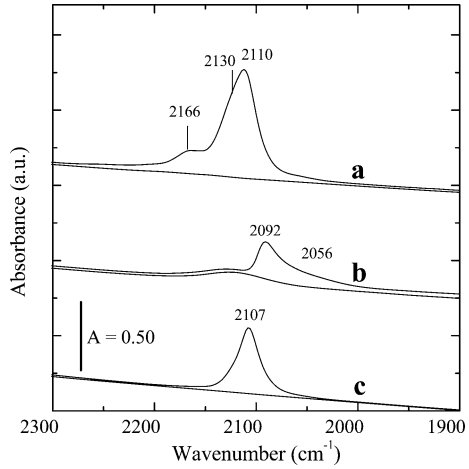

Figure 12. FTIR study of the influence of the pretreatment applied to the Au/CZ catalyst on its CO adsorption capability (P_{CO} = 10 Torr). (a) Sample submitted to the standard oxidation/evacuation treatment at 523 K. (b) Sample reduced/evacuated at 673 K. (c) Sample (b) further reoxidized with 40 Torr of O_2 at 298 K (0.5 h) and evacuated at 298 K (1 h).

toward lower frequencies from 2110 to 2092 cm^{-1}, and its integrated absorption is reduced by a factor of 4.6. As recently discussed in refs 14 and 48, the position of the main band in spectrum b, 2092 cm^{-1}, may be interpreted as due to the occurrence of a significant electron transfer from the reduced support to the Au nanocrystals. In parallel with the frequency shift, we may also notice a very significant loss of the CO adsorption capability. Some sintering of the gold particles is likely to contribute to this deactivation effect. The question, however, is whether the metal/reduced-support interaction plays also a role. The comparative analysis of spectra b and c in Figure 12 has provided us with useful information in this respect. In effect, with reference to spectrum b the ν_{CO} band in spectrum c shifts back toward higher wavenumbers (from 2092 to 2107 cm^{-1}). The position of the latter band, which is rather close to that observed in spectrum a of Figure 12, allows us its assignation to CO adsorbed on neutral Au nanocrystallites.[14,48] Simultaneously, an increase of the integrated absorption by a factor of 2.4 is observed. The metal deactivation induced by the reduction/evacuation pretreatment at 673 K may therefore be partly reverted by reoxidation/evacuation at 298 K. The application of such a very mild treatment should be expected not to modify the gold particle size distribution. Accordingly, both metal sintering and a reversible loss of the CO adsorption capability, associated to the interaction of Au nanocrystals with the reduced support, are likely to contribute to the catalysts deactivation and therefore to the inhibition of the hydrogen spillover in the Au/CZ sample reduced at 673 K.

Conclusions

A 3 wt % Au/$Ce_{0.62}Zr_{0.38}O_2$ catalyst prepared by deposition−precipitation method has been studied. As revealed by electron microscopy (STEM−HAADF and HREM studies), XRD, and the combined application of FTIR and volumetric adsorption of CO, gold is well dispersed on the ceria−zirconia-mixed oxide support. The approach followed in this work, consisting of the joint analysis of FTIR and volumetric data of chemisorbed CO recorded at room temperature, has proven to be a useful tool for a qualitative evaluation of the metal dispersion in this family of ceria-containing gold catalysts.

As deduced from the results presented and discussed here, the catalyst submitted to the standard oxidizing pretreatment

exhibits at room temperature a strong and fast spillover effect. This effect, however, may be very significantly inhibited by CO co-adsorption as well as by a reduction/evacuation pretreatment at 673 K. The recovery from these deactivated states may be achieved by simple evacuation at 298 K in the former case and by a very mild reoxidation treatment with 40 Torr of O_2 at 298 K in the latter.

Finally, the reported results strongly suggest that H_2 and CO adsorptions on our Au/CZ catalyst are competitive processes involving the same gold sites. This would explain the remarkable perturbation induced by the CO on the hydrogen spillover.

Acknowledgment. We thank the financial support from the Ministry of Education and Science of Spain/FEDER Program of the EU (Project MAT2005-00333) and the Junta de Andalucía (Group FQM-110). The ceria−zirconia sample was kindly donated by Grace Davison Company.

Supporting Information Available: XRD diagrams, STEM−HAADF and HREM images, and tables of CO chemisorption on the Au/CZ catalyst, CO chemisorption on the bare CZ support, and H_2 chemisorption on the Au/CZ catalyst. This material is available free of charge via the Internet at http://pubs.acs.org.

References and Notes

(1) Bond, G. C.; Louis, C.; Thompson, D. T. *Catalysis by Gold*; Catalytic Science Series, Vol. 6.; World Scientific Publishing Co.: London, 2006.

(2) Hashmi, A. S. K.; Hutchings, G. J. *Angew. Chem., Int. Ed.* **2006**, *45*, 7896−7936.

(3) Nieuwenhuys, B. E.; Gluhoi, A. C.; Rienks, E. D. L.; Wetstrate, C. J.; Vinod, C. P. *Catal. Today* **2005**, *100*, 49−54.

(4) Hutchings, G. J. *Catal. Today* **2005**, *100*, 55−61.

(5) Haruta, M. *Gold Bull.* **2004**, *37*, 27−36.

(6) Bond, G. C. *Catal. Today* **2002**, *72*, 5−9.

(7) Bond, G. C.; Thompson, D. T. *Catal. Rev.—Sci. Eng.* **1999**, *41*, 319−388.

(8) Haruta, M.; Kobayashi, T.; Sano, H.; Yamada, N. *Chem. Lett.* **1987**, *16*, 405−408.

(9) Haruta, M.; Yamada, N.; Kobayashi, T.; Iiyima, S. *J. Catal.* **1989**, *115*, 301−309.

(10) Hutchings, G. J. *J. Catal.* **1985**, *96*, 292−295.

(11) Haruta, M. *Catal. Today* **1997**, *36*, 153−166.

(12) Haruta, M. *CATTECH* **2002**, *6*, 102−115.

(13) Haruta, M. *Gold Bull.* **2004**, *37*, 27−36.

(14) Manzoli, M.; Boccuzzi, F.; Chiorino, A.; Vindigni, F.; Deng, W.; Flytzani-Stephanopoulos, M. *J. Catal.* **2007**, *245*, 308−315.

(15) Deng, W.; Flytzani-Stephanopoulos, M. *Angew. Chem., Int. Ed.* **2006**, *45*, 2285−2289.

(16) Concepción, P.; Carrettin, S.; Corma, A. *Appl. Catal., A* **2006**, *307*, 42−45.

(17) Kim, C. H.; Thompson, L. T. *J. Catal.* **2006**, *244*, 248−250.

(18) Leppelt, R.; Schumacher, B.; Plzak, V.; Kinne, M.; Behm, R. J. *J. Catal.* **2006**, *244*, 137−152.

(19) Pillai, U. R.; Deevi, S. *Appl. Catal., A* **2006**, *299*, 266−273.

(20) Campo, B.; Volpe, M.; Ivanova, S.; Touroude, R. *J. Catal.* **2006**, *242*, 162−171.

(21) Arena, F.; Famulari, P.; Trunfio, G.; Bonura, G.; Frusteri, F.; Spadaro, L. *Appl. Catal., B* **2006**, *66*, 81−91.

(22) Guzmán, J.; Carrettin, S.; Fierro-González, J. C.; Hao, Y.; Gates, B. C.; Corma, A. *Angew. Chem., Int. Ed.* **2005**, *44*, 4778−4781.

(23) Guzmán, J.; Carrettin, S.; Corma, A. *J. Am. Chem. Soc.* **2005**, *127*, 3286−3287.

(24) Fu, Q.; Deng, W.; Saltsburg, H.; Flytzani-Stephanopoulos, M. *Appl. Catal., B* **2005**, *56*, 57−68.

(25) Deng, W.; Jesus, J. D.; Saltsburg, H.; Flytzani-Stephanopoulos, M. *Appl. Catal., A* **2005**, *291*, 126−135.

(26) Venezia, A. M.; Pantaleo, G.; Longo, A.; Di Carlo, G.; Casaletto, M. P.; Liotta, F. L.; Deganello, G. *J. Phys. Chem. B* **2005**, *109*, 2821−2827.

(27) Kim, C. H.; Thompson, L. T. *J. Catal.* **2005**, *230*, 66−74.

(28) Trimm, D. L. *Appl. Catal., A* **2005**, *296*, 1−11.

(29) Sakurai, H.; Akita, T.; Tsubota, S.; Kiuchi, M.; Haruta, M. *Appl. Catal., A* **2005**, *291*, 179−187.

(30) Carrettin, S.; Concepción, P.; Corma, A.; López-Nieto, J. M.; Puntes, V. F. *Angew. Chem., Int. Ed.* **2004**, *43*, 2538−2540.

(31) Tabakova, T.; Boccuzzi, F.; Manzoli, M.; Andreeva, D. *Appl. Catal., A* **2003**, *252*, 385−397.

(32) Fu, Q.; Saltsburg, H.; Flytzani-Stephanopoulos, M. *Science* **2003**, *301*, 935−938.

(33) Fu, Q.; Kudriavtseva, S.; Saltsburg, H.; Flytzani-Stephanopoulos, M. *Chem. Eng. J.* **2003**, *93*, 41−53.

(34) Fu, Q.; Weber, A.; Flytzani-Stephanopoulos, M. *Catal. Lett.* **2001**, *77*, 87−95.

(35) Bernal, S.; Kaspar, J.; Trovarelli, A. *Catal. Today* **1999**, *50*, 173−443.

(36) *Catalysis by Ceria and Related Materials*; Trovarelli, A., Ed.; Catalytic Science Series, Vol. 2.; Imperial College Press: London, 2006.

(37) Tibiletti, D.; Amieiro-Fonseca, A.; Burch, R.; Chen, Y.; Fisher, J. M.; Goguet, A.; Hardacre, C.; Hu, P.; Thompsett, D. *J. Phys. Chem. B* **2005**, *109*, 22553−22559.

(38) Radhakrishnan, R.; Willigan, R. R.; Dardas, Z.; Vanderspurt, T. H. *AIChE J.* **2006**, *52*, 1888−1894.

(39) Bond, G. C.; Thompson, D. T. *Appl. Catal., A* **2006**, *302*, 1−4.

(40) Bernal, S.; Calvino, J. J.; Gatica, J. M.; López-Cartes, C.; Pintado, J. M. Chemical and Nanostructural Aspects of the Preparation and Characterisation of Ceria and Ceria-Based Mixed Oxide Supported Metal Catalysts. In *Catalysis by Ceria and Related Materials*; Trovarelli, A., Ed; Imperial College Press: London, 2002; Chapter 4, pp 85−168.

(41) Yeste, M. P.; Hernández, J. C.; Bernal, S.; Blanco, G.; Calvino, J. J.; Pérez-Omil, J. A.; Pintado, J. M. *Chem. Mater.* **2006**, *18*, 2750−2757.

(42) Norman, A.; Perrichon, V.; Bensaddik, A.; Lemaux, S.; Bitter, H.; Koningsberger, D. *Top. Catal.* **2001**, *16/17*, 363.

(43) Hickey, N.; Fornasiero, P.; Kaspar, J.; Gatica, J. M.; Bernal, S. *J. Catal.* **2001**, *200*, 181−193.

(44) Gatica, J. M.; Baker, R. T.; Fornasiero, P.; Bernal, S.; Blanco, G.; Kaspar, J. *J. Phys. Chem. B* **2000**, *104*, 4667−4672.

(45) Zanella, R.; Giorgio, S.; Henry, C. R.; Louis, C. *J. Phys. Chem. B* **2002**, *106*, 7634−7642.

(46) Menegazzo, F.; Manzoli, M.; Chiorino, A.; Boccuzzi, F.; Tabakova, T.; Signoretto, M.; Pinna, F.; Pernicone, N. *J. Catal.* **2006**, *237*, 431−434.

(47) Margitfalvi, J. L.; Fasi, A.; Hegedus, M.; Lonyi, F.; Gobolos, S.; Bogdanchikova, N. *Catal. Today* **2002**, *72*, 157−169.

(48) Chen, M.; Goodman, D. W. *Acc. Chem. Res.* **2006**, *39*, 739−746.

(49) Daturi, M.; Binet, C.; Lavalley, J.-C.; Galtayries, A.; Sporken, R. *Phys. Chem. Chem. Phys.* **1999**, *1*, 5717−5724.

(50) Daturi, M.; Binet, C.; Lavalley, J.-C.; Blanchard, G. *Surf. Interface Anal.* **2000**, *30*, 273−277.

(51) Derrouiche, S.; Gravejat, P.; Bianchi, D. *J. Am. Chem. Soc.* **2004**, *126*, 13010−13015.

(52) Meier, D. C.; Bukhtiyarov, V.; and Goodman, D. W. *J. Phys. Chem. B* **2003**, *107*, 12668 − 12671.

(53) Meier, D. C.; Goodman, D. W. *J. Am. Chem. Soc.* **2004**, *126*, 1892−1899.

(54) Vidal, H.; Kaspar, J.; Pijolat, M.; Colon, G.; Bernal, S.; Cordón, A.; Perrichon, V.; Fally, F. *Appl. Catal., B* **2000**, *27*, 49−63.

(55) Andreeva, D.; Idakiev, V.; Tabakova, T.; Ilieva, L.; Falaras, P.; Bourlinos, A.; Travlos, A. *Catal. Today* **2002**, *72*, 51−57.

(56) Tabakova, T.; Boccuzzi, F.; Manzoli, M.; Sobczak, J. W.; Idakiev, V.; Andreeva, D. *Appl. Catal., A* **2006**, *298*, 127−143.

(57) Daturi, M.; Finocchio, E.; Binet, C.; Lavalley, J.-C.; Fally, F.; Perrichon, V. *J. Phys. Chem. B* **1999**, *103*, 4884−4891.

(58) Pokrovski, K. A.; Bell, A. T. *J. Catal.* **2006**, *241*, 276−286.

(59) Finocchio, E.; Daturi, M.; Binet, C.; Lavalley, J.-C.; Blanchard, G. *Catal. Today* **1999**, *52*, 53−63.

(60) Gennari, F. C.; Montini, T.; Hickey, N.; Fornasiero, P.; Graziani, M. *Appl. Surf. Sci.* **2006**, *252*, 8456−8465.

(61) Gluhoi, A. C.; Vreburg, H. S.; Bakker, J. W.; Nieuwenhuys, B. E. *Appl. Catal., A* **2005**, *291*, 145−150.

(62) Boccuzzi, F.; Chiorino, A.; Manzoli, M.; Andreeva, D.; Tabakova, T. *J. Catal.* **1999**, *188*, 176−185.

(63) Bus, E.; Miller, J. T.; van Bokhoven, J. A. *J. Phys. Chem. B* **2005**, *109*, 14581−14587.

(64) Binet, C.; Badri, A.; Lavalley, J.-C. *J. Phys. Chem.* **1994**, *98*, 6392−6398.

(65) Bernal, S.; Calvino, J. J.; Cifredo, G. A.; Rodríguez-Izquierdo, J. M.; Perrichon, V.; Laachir, A. *Chem. Commun.* **1992**, 460−462

(66) Bernal, S.; Calvino, J. J.; Cifredo, G. A.; Rodríguez-Izquierdo, J. M. *J. Phys. Chem.* **1995**, *99*, 11794−11796.

(67) Madier, Y.; Descorme, C.; Le Govic, A. M.; Duprez, D. *J. Phys. Chem. B* **1999**, *103*, 10999−11006.

(68) Phala, N. S.; Klatt, G.; van Stee, E. *Chem. Phys. Lett.* **2004**, *395*, 33−37.